Journal of Alloys and Compounds 509 (2011) 8885–8887

Contents lists available at ScienceDirect

Journal of Alloys and Compounds

journal homepage: www.elsevier.com/locate/jallcom

Electric field-modulated Hall resistivity and magnetization in magnetoelectric Ni–Mn–Co–Sn/PMN–PT laminate

S.Y. Chen [a,b], Y.X. Zheng [a], Q.Y. Ye [b], H.C. Xuan [a], Q.Q. Cao [a], Y. Deng [c], D.H. Wang [a,*], Y.W. Du [a], Z.G. Huang [b]

[a] National Laboratory of Solid State Microstructures and Key Laboratory of Nanomaterials for Jiang Su Province, Department of Physics, Nanjing University, Nanjing 210093, People's Republic of China

[b] Department of Physics, Fujian Normal University, Fuzhou 350007, People's Republic of China

[c] Centre of Materials Analysis, Nanjing University, Nanjing 210093, People's Republic of China

ARTICLE INFO

Article history:
Received 15 November 2010
Received in revised form 13 May 2011
Accepted 16 May 2011
Available online 30 June 2011

Keywords:
Magnetoelectric composite
Ferromagnetic shape memory alloy
Hall resistivity
Electric field modulation

ABSTRACT

The effects of electric field on the magnetization and Hall resistivity were investigated in a laminated composite consisting of $Ni_{43}Mn_{41}Co_5Sn_{11}$ alloy and $Pb(Mg_{1/3}Nb_{2/3})O_3$–$PbTiO_3$ ferroelectric single crystal. Upon applying an electric field (3 kV/cm) on the single crystal, the change of Hall resistivity in the alloy is up to 45%. The co-action of magnetization change and the different carrier concentration between the martensitic and austenite phases of alloy, which result from the stress-induced martensitic transformation, are responsible for the electric field-modulated Hall resistivity.

© 2011 Elsevier B.V. All rights reserved.

1. Introduction

The control of magnetization, which is an important issue in technological applications, has commonly been accomplished by a current-generated magnetic field. This method is disadvantage for reducing power consumption and realizing device miniaturization. So the manipulation of magnetization by other means is highly desired. Recently, the topic that electric field modulates magnetic properties directly in magnetoelectric composites are particularly appealing [1–6], for example, electric field-modulated magnetism has been achieved in some magnetoelectric laminates consisting of ferromagnetic phase and ferroelectric one [1,7–9], such as FeCoV/PZN–PT and Metglas/PMN–PT laminated composites, in which electric-field modulated magnetization change up to 80% was obtained [9]. However, these investigations have mostly focused on the magnetization change (ΔM) of ferromagnetic phase, which is controlled by an electric field. Due to the variation of the magnetic properties in ferromagnetic phase, the magnetic transport properties, such as Hall resistivity (ρ_H) and magnetoresistance (MR), would change correspondingly. Therefore, the electric field-modulated ρ_H or MR may be realized in magnetoelectric composites. This alternative modulation is attractive for advanced applications, since it provides an additional freedom of degree in the design of spintronic devices.

Ferromagnetic shape memory alloy (FSMA) is a kind of multifunctional material, which shows ferromagnetism and shape memory effect simultaneously. Recently, a series of Ni–Mn–X (X = In, Sn, Sb and Ga) FSMAs have been extensively investigated for their interesting physical properties associated with the martensitic transformation (MT), such as magnetic field-induced shape recovery [10], giant magnetocaloric effect [11,12], large MR [13] and Hall effect [14]. It is well known that the MT in these alloys can be driven by temperature, magnetic field and stress, resulting in the change of magnetization. By utilizing this property, large magnetoelectric effect has been obtained in FSMA/PZT laminated composites [15,16]. As mentioned above, it is valuable to study the effect of electric field on the magnetic transport properties in these magnetoelectric composites. But up to now, seldom work had been done to investigate the issue [17]. In this work, the effect of electric field on Hall effect in a $Ni_{43}Mn_{41}Co_5Sn_{11}$ (NMCS)/$Pb(Mg_{1/3}Nb_{2/3})O_3$–$PbTiO_3$ (PMN–PT) laminate composite was investigated. The results indicate that the ρ_H change up to 45% in NMCS alloy can be obtained by applying an electric field of 3 kV/cm on ferroelectric phase in NMCS/PMN–PT laminate composite, the experimental results presented in this paper provide an alternative modulation for Hall effect, which is usually controlled by magnetic field in a given material, such as magnetic semiconductor, half-metallic material, and so on.

2. Materials and methods

Polycrystalline NMCS alloy was prepared using conventional arc melting techniques in an argon atmosphere, in which commercially available Ni, Mn, Co and

* Corresponding author. Tel.: +86 25 83594588; fax: +86 25 83594588.
E-mail address: wangdh@nju.edu.cn (D.H. Wang).

0925-8388/$ – see front matter © 2011 Elsevier B.V. All rights reserved.
doi:10.1016/j.jallcom.2011.05.058

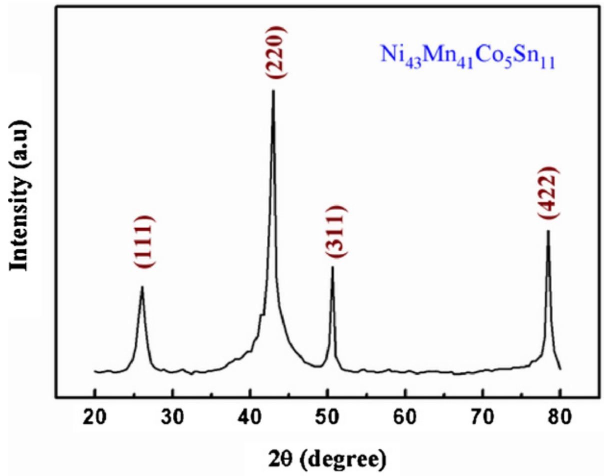

Fig. 1. X-ray pattern of $Ni_{43}Mn_{41}Co_5Sn_{11}$ alloy at room temperature.

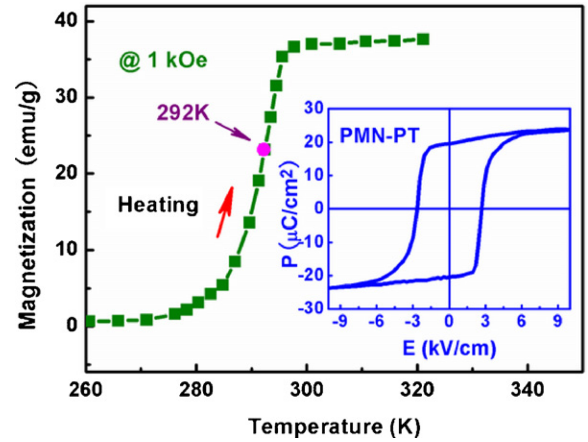

Fig. 3. Thermo-magnetization curve for NMCS alloy at $H = 1$ kOe. The inset shows the ferroelectric hysteresis loop of PMN–PT crystal at room temperature.

Sn of 4N purity were used. For homogenization, the elements were melted four times, and then the NMCS alloy was annealed at 1173 K for 96 h, followed by a quenching in water. X-ray diffraction (XRD) was carried out to examine the crystal structure of the alloy. X-ray pattern shown in Fig. 1 indicates that a cubic Heusler $L2_1$ (austenite) structure NMCS alloy was obtained. Then, the NMCS/PMN–PT laminated composite was prepared by epoxy bonding the polarized PMN–PT chip with NMCS alloy slice. Here, (0 0 1)-cut ferroelectric single crystal PMN–PT (polarized along [0 0 1] direction) with d_{31} about −1900 pC/N was commercially supplied. The schematic illustration of this laminate structure is shown in Fig. 2. Magnetic properties were measured using a vibrating sample magnetometer (Lakeshore 7400). Hall effect measurement was performed in square (5 mm × 5 mm) using a system combining precision current source (Keithlkey 6220) with nanovoltmeter (Keithley 2182A) by the van der Pauw method [18]. The geometry configuration of the measurement is also shown in Fig. 2. The thickness of NMCS alloy and PMN–PT crystal was 0.1 and 1.0 mm, respectively. In the case of Hall effect measurement, the external magnetic field (H) was applied along thickness direction. The contribution from offset values or MR effect was carefully removed by changing the direction of magnetic field.

Considering the practical application, the MT temperature of NMCS alloy was carefully adjusted to room temperature based on the correlation between MT and the valence electron concentration e/a (the number of electron per atom) in Ni–Mn based FSMAs [19]. The thermomagnetic property of NMCS alloy was investigated at $H = 1$ kOe, as shown in Fig. 3. On heating, the alloy undergoes a reverse MT from weak magnetic martensitic phase to ferromagnetic austenitic phase near 292 K, where an abrupt change of magnetization is observed. The inset of Fig. 3 shows the ferroelectric hysteresis loop of PMN–PT single crystal and the electric coercivity (E_c) is about 2.9 kV/cm.

3. Results and discussion

Fig. 4 shows the initial magnetization curves of NMCS with different electric field applying *in situ* on PMN–PT ceramic. From the inset (a) of Fig. 4, it is obvious that the application of electric field on the ceramic results in the remarkable shift in magnetization curves.

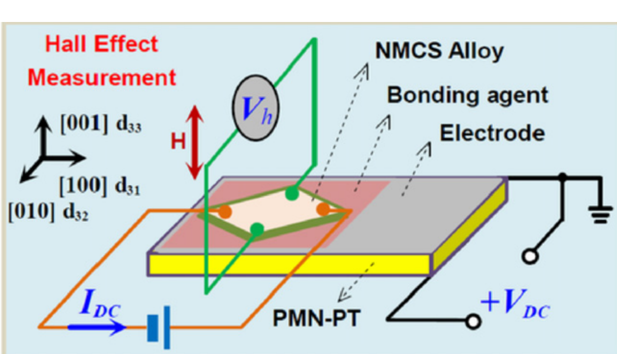

Fig. 2. Schematic illustration of the structure of NMCS/PMN–PT laminate and Hall effect measurement.

It is well known that the applied electric field on PMN–PT crystal would produce a stress due to the reverse piezoelectric effect. This stress then transfers to NMCS alloy and gives rise to ΔM due to the stress-induced MT in FSMA [20].

For further understanding the relationship between ΔM and electric field, the magnetization of the laminate at $H = 5$ kOe as a function of electric field is shown in the inset (b) of Fig. 4. It is obvious that the magnetization first increases with increasing electric field and reaches a maximum around E_c of PMN–PT. Then it decreases with increasing electric field. When electric field is up to 8 kV/cm, the magnetization is even less than that at zero electric field. As mentioned above, the stress-driven MT in NMCS alloy results in the variation of magnetization, so the electric field-induced strain in PMN–PT crystal would be responsible for the ΔM in the laminate. In our measurement, PMN–PT single crystal was polarized along [0 0 1] direction beforehand. An electric field, which direction was opposite to that of remnant polarization of PMN–PT single crystal, was then applied on the ceramic. According to the hysteresis between strain and electric field [21], the strain would first increase with the increasing electric field and reach a maximum value around E_c, which can be verified by the experimental result that the magnetization at 3 kV/cm is the largest. At larger electric field, due to the strain remanence, the switching of

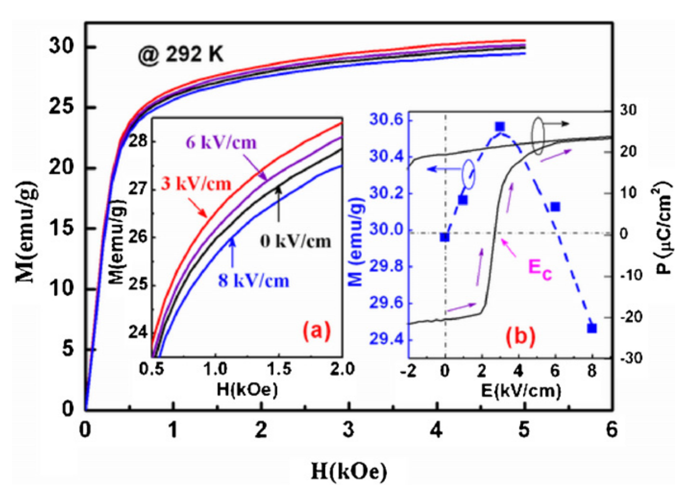

Fig. 4. The initial magnetization curves for NMCS alloy at different electric fields. Inset (a) shows the expanded view of initial magnetization curves in the range of 0.5–2.0 kOe; inset (b) presents the electric field dependence of magnetization for NMCS/PMN–PT laminate at $H = 5$ kOe (square solid dots), where the dashed line is a guide to the eye. Solid line shows the ferroelectric hysteresis loop of PMN–PT crystal.

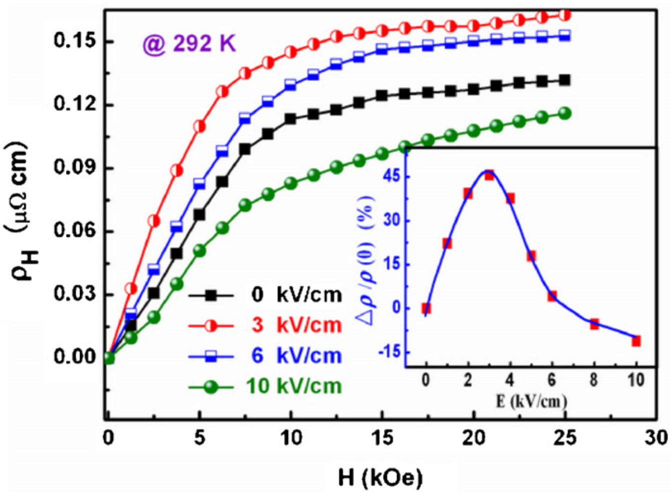

Fig. 5. ρ_H as a function of H at different electric fields. The inset shows the electric field dependence of $\Delta\rho_H/\rho_H$ for NMCS/PMN–PT laminate at H = 5 kOe (square solid dots), where the solid line is a guide to the eye.

the polarization does not make the strain reverse immediately, i.e. the strain would decrease to zero with increasing electric field and then change its direction at a high enough electric field [21]. The reversed strain would give rise to a negative change of the magnetization. This result is ascribed to the fact that the tensile stress and the compressive stress, which are produced by the strain with different direction, have reverse effect on driving MT and then result in the opposite ΔM in NCMS alloy.

Fig. 5 presents the magnetic field dependence of ρ_H for NMCS/PMN–PT laminate with different electric field applying on PMN–PT crystal. As we know, ρ_H in magnetic materials can be expressed as following [22]:

$$\rho_H = R_0 B_Z + R_A 4\pi M_Z \quad (1)$$

where the first term describes the ordinary Hall effect and R_0 is ordinary Hall coefficient. The second term presents the anomalous Hall resistivity related to the magnetization, which is considered to originate from spin-orbit interactions [22] or Berry phase of the Bloch electrons [23], here R_A is anomalous Hall coefficient. Generally, the anomalous Hall effect is dominant in magnetic materials, in which R_A is much higher than R_0 [23]. As shown in Fig. 5, it is obvious that ρ_H first increases quickly with increasing H up to about 10 kOe, and then a gentle increase of ρ_H is observed, which is attributed to the saturation tendency of magnetization under higher external magnetic field. It is worth noting that the values of ρ_H vary with different electric field, showing a remarkable modulated Hall effect. As shown in the inset of Fig. 5, the maximum change of $\Delta\rho_H/\rho_H$, which is defined as $[\rho_H(E) - \rho_H(0)]/\rho_H(0)$, is up to 45% at 3 kV/cm and 5 kOe. According to Eq. (1), ρ_H should increase with increasing magnetization, which can be reflected by the fact that the electric field dependence of ρ_H is identical to that of magnetization. Since MT is a first-order phase transition between martensite and austenite, the effect of the structural transition on ρ_H should be considered as well. Actually, the first-order MT in Ni–Mn-based FSMAs often develops with a region of metastability with austenite and martensite coexisting, especially around MT temperature [24,25]. During the structural transition, more and more austenitic (or martensitic) fractions transfer into martensitic (or austenitic) phases. As we know, the carrier concentration of martensitic phase is different from that of austenitic phase, which would lead to the variation of R_A. Therefore, the two contributions from the changes of magnetization and carrier concentration, which are realized by the stress-induced MT in NMCS, would account for the electric filed-modulated Hall effect in the laminate.

4. Conclusions

In summary, electric field-modulated magnetic and transport properties were investigated in a laminated NMCS/PMN–PT magnetoelectric composite. The experimental results indicated that the magnetization, as well as ρ_H in NMCS alloy, could be well controlled by applying different electric field on PMN–PT crystal. Under H = 5 kOe, the maximum change of ρ_H up to 45% was obtained by applying an electric field of 3 kV/cm on PMN–PT single crystal. The mechanism of stress-induced MT in FSMA and thereby, the changes of magnetization and carrier concentration, would be responsible for the variation of ρ_H in the laminate. This additional control pattern for Hall effect in magnetoelectric composite suggests the promising potential in the technological application of sensors and some precise measurements.

Acknowledgements

This work is supported by the National Natural Science Foundation of China (50701022, 50971069, 11004031 and 50802039), the Program for New Century Excellent Talents of China (NCET-08-0278, NCET-08-0631), Natural Science Foundation and Education Office Foundation of Fujian Province (2010J01277 and JA10086).

References

[1] M. Gajek, M. Bibes, S. Fusil, K. Bouzehouane, J. Fontcuberta, A. Barthelemy, A. Fert, Nat. Mater. 6 (2007) 296.
[2] W. Eerenstein, M. Wioral, J.L. Prieto, J.F. Scott, D. Mathur, Nat. Mater. 6 (2007) 348.
[3] Y.H. Chu, L.W. Martin, M.B. Holcomb, G. Martin, S.J. Han, Q. He, N. Balke, C.H. Yang, D. Lee, W. Hu, Q. Zhan, P.L. Yang, A.F.I. Guez, A. Scholl, S.X. Wang, R. Ramesh, Nat. Mater. 7 (2008) 478.
[4] F. Zavaliche, T. Zhao, H. Zheng, F. Straub, M.P. Cruz, P.L. Yang, D. Hao, R. Ramesh, Nano Letters 7 (2007) 1586.
[5] J. Ma, Y.H. Lin, C.-W. Nan, J. Phys. D: Appl. Phys. 43 (2010) 12001.
[6] V. Garcia, M. Bibes, L. Bocher, S. Valencia, F. Kronast, A. Crassous, X. Moya, S. Enouz-Vedrenne, A. Gloter, D. Mhoff, D. Deranlot, N.D. Mathur, S. Fusil, K. Bouzehouane, A. Barthélémy, Science 327 (2010) 1106.
[7] Y.J. Chen, J.S. Gao, T. Fitchorov, Z.H. Cai, K.S. Ziemer, C. Vittoria, V.G. Harris, Appl. Phys. Lett. 94 (2009) 082504.
[8] J.P. Zhou, Y.Y. Guo, Z.Z. Xi, P. Liu, S.Y. Lin, G. Liu, H.W. Zhang, Appl. Phys. Lett. 93 (2008) 152501.
[9] Y.J. Chen, A.L. Geiler, T. Fitchorov, C. Vittoria, V.G. Harris, Appl. Phys. Lett. 95 (2009) 182501.
[10] Y. Sutou, Y. Imano, N. Koeda, T. Omori, R. Kainuma, K. Ishida, K. Oikawa, Appl. Phys. Lett. 85 (2004) 4358.
[11] Z.D. Han, D.H. Wang, C.L. Zhang, H.C. Xuan, B.X. Gu, Y.W. Du, Appl. Phys. Lett. 90 (2007) 042507.
[12] T. Krenke, E. Duman, M. Acet, E.F. Wassermann, X. Moya, L. Mañosa, A. Planes, Nat. Mater. 4 (2005) 450.
[13] S.Y. Yu, L. Ma, G.D. Liu, Z.H. Liu, J.L. Chen, Z.X. Cao, G.H. Wu, B. Zhang, X.X. Zhang, Appl. Phys. Lett. 90 (2007) 242501.
[14] Z.Y. Zhu, S.W. Or, G.H. Wu, Appl. Phys. Lett. 95 (2009) 032503.
[15] Y.J. Chen, M. Liu, J. Lou, N.X. Sun, C. Vittoria, V.G. Harris, Appl. Phys. Lett. 93 (2008) 112502.
[16] S.Y. Chen, D.H. Wang, Z.D. Han, C.L. Zhang, Y.W. Du, Z.G. Huang, Appl. Phys. Lett. 95 (2009) 022501.
[17] R.K. Zheng, Y. Wang, J. Wang, K.S. Wong, H.L.W. Chan, C.L. Choy, H.S. Luo, Phys. Rev. B 74 (2003) 094427.
[18] L.J. van der Pauw, Philips Tech. Rev. 20 (1958) 220.
[19] J. Marcos, L. Mañosa, A. Planes, F. Casanova, X. Batlle, A. Labarta, Phys. Rev. B 68 (2003) 094401.
[20] S. Kustov, M. Corró, E. Cesari, Appl. Phys. Lett. 91 (2007) 141907.
[21] D. Damjanovic, Rep. Prog. Phys. 61 (1998) 1267.
[22] Z. Fang, N. Nagaosa, K.S. Takahashi, A. Asamitsu, R. Mathieu, T. Ogasawara, H. Yamada, M. Kawasaki, Y. Tokura, K. Terakura, Science 302 (2003) 92.
[23] D. Venkateshvaran, W. Kaiser, A. Boger, M. Althammer, M.S.R. Rao, Phys. Rev. B 78 (2008) 092405.
[24] S. Chatterjee, S. Giri, S. Majumdar, A.K. Deb, S.K. De, V. Hardy, J. Phys.: Condens. Matter 19 (2007) 346213.
[25] S. Chatterjee, S. Giri, S. Majumdar, S.K. De, Phys. Rev. B 77 (2008) 012404.